J. Geogr. Sci. 2020, 30(6): 935-948
DOI: https://doi.org/10.1007/s11442-020-1763-2

Using water isotopes and hydrogeochemical evidences to characterize groundwater age and recharge rate in the Zhangjiakou area, North China

ZHANG Qinghua[1], *LUO Zhuanxi[1], LU Wen[3], HARALD Zepp[4], ZHAO Yufeng[1,2], TANG Jialiang[3]

1. Key Laboratory of Urban Environment and Health, Institute of Urban Environment, CAS, Xiamen 361021, Fujian, China;
2. College of Geographical Science, Shanxi Normal University, Linfen 041000, Shanxi, China;
3. Institute of Mountain Hazards and Environment, CAS, Chengdu 610041, China;
4. Geographical Institute, Ruhr-University Bochum, Bochum D-44780, Germany

Abstract: Despite the increasing depletion of the groundwater at the Zhangjiakou aquifer system in the northwest of Beijing-Tianjin-Hebei region, little information is available on the hydrological process of groundwater in this region. In this study, we utilized water isotopes composition ($\delta^{18}O$, δD and ^{3}H) of groundwater, river and precipitation to identify the characteristics of hydrochemistry, groundwater age and recharge rates in different watersheds of the Zhangjiakou area. Results showed that the river water and groundwater could be characterized as HCO_3-Mg·Na, HCO_3·Cl-Na and HCO_3-Mg·Na, HCO_3·Cl-Na, HCO_3·Cl-Na·Mg types, respectively. The δD and $\delta^{18}O$ values in precipitation were linearly correlated, which is similar to the Global Meteorological Water Line (GMWL). Furthermore, the decreasing values of the δD and $\delta^{18}O$ from precipitation to surface water and groundwater indicate that groundwater is mainly recharged by atmospheric precipitation. In addition, the variation of ^{3}H concentration with depth suggests that groundwater shallower than around 100 m is generally modern water. In contrast, groundwater deeper around 100 m is a mixture of modern and old waters, which has longer residence times. Groundwater showed a relatively low tritium concentration in the confined aquifers, indicating the groundwater recharged might be relatively old groundwater of over 60 years. The flow velocity of the groundwater in the study area varied from 1.10 to 2.26 m/a, and the recharge rates ranged from 0.034 to 0.203 m/a. The obtained findings provide important insights into understanding the groundwater recharge sources and hydrochemistry in the Zhangjiakou area, in turn developing a sustainable groundwater management plan.

Keywords: hydrogen and oxygen isotopes; tritium isotope; water cycle; groundwater; Zhangjiakou

Received: 2019-09-20 **Accepted:** 2020-03-05
Foundation: The National Major Science and Technology Program for Water Pollution Control and Treatment, No. 2017ZX07101001-02
Author: Zhang Qinghua (1990–), MS Candidate, specialized in environmental geochemistry. E-mail: tsinghua_cags@163.com
***Corresponding author:** Luo Zhuanxi (1979–), PhD, E-mail: zxluo@iue.ac.cn; zxluoire@163.com

1 Introduction

Groundwater is an important water resource in arid and semi-arid regions, and the widespread over-exploitation of groundwater is a global issue (Foster and Chilto *et al*., 2003; Wada *et al*., 2012; Dollet *et al*., 2012; Gleeson *et al*., 2015). The global groundwater exploitation rate was estimated at about 1500 km^3 per year, which was much larger than the natural recharge rate of groundwater (Dollet *et al*., 2012). This problem has become more severe with increasing population growth and lack of understanding of the regional water cycle. Surface water and groundwater are important components of the water cycle in a basin (Kalbus *et al*., 2006). Clearly, understanding of the mutual transformation between surface water and groundwater is critical to utilize scientifically water resources in any basin.

The measurements of water isotopes ($\delta^{18}O$, δD and ^3H) combined with hydrochemical evidences are effective ways to study the water cycle. The tracing techniques play an important role in the study of groundwater recharge sources and mutual conversion between surface water and groundwater in a basin (Perry *et al*., 2009; Huang *et al*., 2010; Li *et al*., 2015; Yao *et al*., 2016; Xu *et al* 2017). Firstly, hydrogen-oxygen stable isotopes (δD and $\delta^{18}O$) are widely used in the research of hydrological cycles in natural and urban environments for better water resources management (Yi *et al*., 2010; Yuan and Mayer 2012; Gibsor 2016; Tipple *et al*., 2017). Furthermore, radioisotopes (^3H) are commonly used in groundwater dating which is important for groundwater management. They are part of water molecules (HTO) and are effective tracers for modern hydrological processes over the past 60 years. Groundwater age can be used to determine groundwater recharge areas, recharge rates, estimate velocities and describe flow characteristics (Liu *et al*., 2014; Kamtchueng *et al*., 2015; Cao *et al*., 2018). Groundwater age is also an effective and informative way to map groundwater renewability and to describe resource attributes, thus facilitating the sustainable use of groundwater resources (Huang *et al*., 2017; Zhang *et al*., 2017). ^3H is also used to calculate groundwater recharge rates and renewability (Morgenstern and Daughney, 2012; Yangui *et al*., 2012; Gusyev *et al*., 2016; Ansari *et al*., 2017).

Until now, previous research on groundwater utilization in China mainly concentrated on the North China Plain and the arid regions in the northwest. Zhangjiakou is located at the intersection of the North China Plain, Mongolian Plateau and Loess Plateau. It is also an important ecological conservation area and water source for Beijing and Tianjin, with the function of balancing natural ecology (Tian *et al*., 2012). The water resources of Zhangjiakou are mainly replenished by atmospheric precipitation, decreasing rainfall during the last 20 years caused repeated droughts and serious water resource crisis in this area. In recent years, with the rapid development of social economy, the gap between the demand for water and the shortage of water resources has become increasingly tremendous. The utilization of surface water resources has been unable to meet the development needs of Zhangjiakou city, thus increasing the exploitation and utilization of groundwater. According to the survey, at present, 70% of the groundwater in the Zhangjiakou area is used for agricultural irrigation purposes, most of which is the results of Cao *et al*. (2019). The shortage of water resources and the irrational utilization have become the most important challenge to the sustainable development of Zhangjiakou's economy.

However, only a few studies have been done on the groundwater recharge and circulation

processes in the Zhangjiakou aquifer system where is mainly in the upper reaches of the Yongding River, which provide a broad understanding of the mechanism of local recharge sources and zones (Chen *et al*., 2017; Feng *et al*., 2013; Hou *et al*., 2019). Even the previous studies of Wang *et al*. (2015) and Li *et al*. (2017) in the upper Yongding river basin did not reach a concensus how fast the groundwater is replenished in this area, Thus, in order to understand the recharge mechanism and spatial characteristics of the aquifer as well as the relationship between surface water and groundwater in the study area, we focused on a region-wide survey for groundwater recharging characteristics in Zhangjiakou, including Zhangbei, Yanghe and Sanggan river basins, based on an integrated tracing approach. This case study was specifically relevant to the sustainable development of the northwestern part of Beijing-Tianjin-Hebei region.

Accordingly, the objectives of this study were (1) to investigate water chemical composition characteristics and water isotope spatial composition characteristics of surface water and groundwater, (2) to calculate the residence time of the groundwater in Zhangjiakou area, (3) to estimate the main recharge sources of groundwater and the transformation relationship between surface water and groundwater. The findings will provide further understanding of the regional water cycle to benefit the rational utilization of water resources in the northwestern part of Beijing-Tianjin-Hebei region.

2 Study area

Zhangjiakou City is located in the northwestern part of Hebei Province, bordering Inner Mongolia Autonomous Region in the north and west, bordering Shanxi Province in the southwest, and connecting Chengde city, Beijing municipality and Baoding city in the east and southeast. The geographical range is between 113°50′–116°30′ E and 39°30′–42°10′N. Zhangjiakou city is 289.2 km long from north to south and 216.2 km wide from east to west. It covers an area of about 36,965 km^2, including 23,149 km^2 in the Bashang plateau and 13,816 km^2 in the Baxia plain. The terrain is relatively flat with an elevation of about 1400 m. The area beyond Bashang plateau accounts for about two-thirds of the total study area. There are many large mountains with altitudes ranging 1000–2000 m. The mountains in the area are formed by a structural cut to form beaded inter-montane basins. The altitudes of the basins range from 500 m to 1000 m. The larger ones are: Chaigoubao-Xuanhua Basin, Yuxian-Yangyuan Basin, and Zhulu-Huailai Basin. There are large rivers in each basin, and relatively fertile cultivated land is distributed in the basins (Sun *et al*., 2014). The study area is located in the mid-latitude area and belongs to the cold temperate continental monsoon climate. It is windy and rainy in spring and autumn, long and cold in winter, and short and hot in summer. The average annual temperature in the whole district is 5–6℃, and the rainfall mostly concentrates in July-August of each year (Shao *et al*., 2012). The average annual precipitation is 403.1 mm with the average evaporation of 1446.9 mm.

The Zhangjiakou area is located in the Yanliao stratigraphic belt. From the old to the new exposures, there are the Archean, Proterozoic, Cambrian, Ordovician, Carboniferous, Permian, Triassic, Jurassic, Tertiary, and Quaternary strata. The lithology revealed in the Bashang plateau is mainly Holocene alluvial deposits, Late Paleozoic granites, and ancient Paleogene Shiji group red clay; the main lithology of the Yanghe river basin is the Upper Pleistocene Malan

Formation and the Late Jurassic granite, Middle Jurassic Anshan Formation, and volcanic breccia; the Sanggan river basin mainly exposes Quaternary alluvial deposits, the Middle Jurassic Anshan Formation and volcanic breccia; the main exposed lithology of the Qingshui river basin is Jurassic andesite, volcanic breccia, schist and marble.

3 Materials and methods

3.1 Sampling and chemical analysis

In order to study the interaction between surface and groundwater in the study area, we determined sampling points based on existing hydrogeological maps and our field surveys (Figure 1). We collected samples from river water, precipitation and groundwater in July 2018 (rainy season), October 2018 (dry season) and April 2019 (snowmelt), respectively. We took 9 samples from the Bashang plateau (Zhangbei), 76 samples from the Qingshui river basin, 36 samples from the Yanghe river basin and 12 samples from the Sanggan river basin. A total of 133 samples were collected in this study, 52 of them are precipitation samples (they were all collected from the Chongli and Chaigoubaodong hydrological monitoring stations), 54 of them are groundwater samples and 27 are surface water samples. However, only the groundwater samples collected in the rainy season are selected to analyze the concentration characteristics of tritium isotope. The groundwater was divided into shallow groundwater (<60 m) and deep groundwater (>60 m) for sampling. Most of the groundwater samples collected in this study were from the deep groundwater due to few shallow groundwater existed. Before sampling, water was released for 30 min using a pump. All water samples were collected in pre-cleaned polypropylene bottles (20 mL for stable isotopic analysis and 500 mL for tritium analysis), and then protected from radiation. Additional parameters, such as pH, temperature (T), electrical conductivity (EC, automatic temperature compensation to 25℃) and total dissolved solids (TDS) were measured in the field using French PONSEL portable multi-parameter water quality instrument. The precision reached 0.01 units, 0.1℃, and 1 μs cm^{-1} for EC. HCO_3^- concentration was measured by the alkalinity meter of Merck Company in Germany. Before titration, samples were percolated with a 0.22 μm aqueous phase needle filter. Each sample was titrated for 2–3 times with an average error of < 5% and an accuracy of 0.1 $mmol \cdot L^{-1}$.

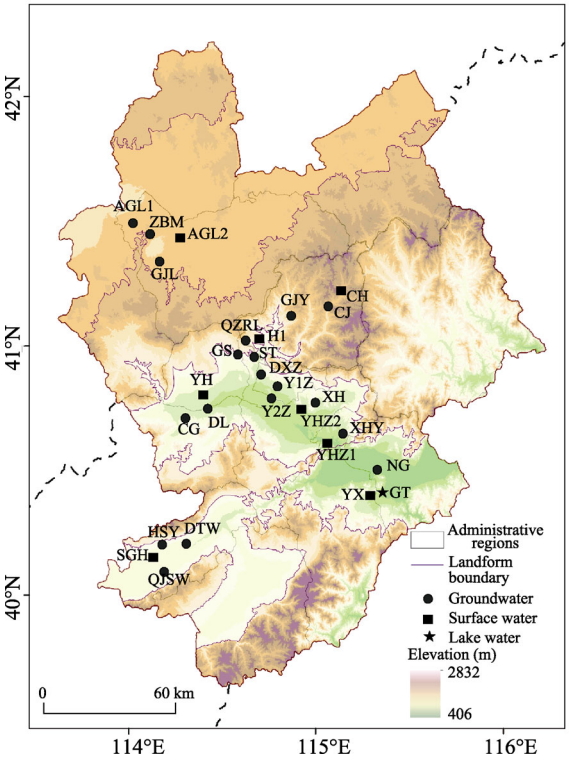

Figure 1 Sampling locations in the Zhangjiakou area

The samples were placed in a refrigerator at 4℃ before testing. The analysis of oxygen and hydrogen isotopes (δD, $\delta^{18}O$) was carried out by L2140-i liquid water vapor isotope analyzer (Picarro, USA). The analysis errors of δD and $\delta^{18}O$ were less than 0.5‰ and 0.1‰ respectively, and the results were given relative to V-SMOW (Vienna Standard Mean Ocean Water) standard. Anions (SO_4^{2-}, Cl^-, NO_3^-, F^-) were analyzed by Dionex ICS3000 ion chromatograph with an accuracy of 0.01 $mg \cdot L^{-1}$, while cations (K^+, Na^+, Ca^{2+}, Mg^{2+}) were analyzed by Aquion ICS ion chromatograph (Thermo Fisher, USA) with an accuracy of 0.01 $mg \cdot L^{-1}$. Furthermore, the tritium isotope (^3H) was analyzed at the Institute of Karst Geology, Chinese Academy of Geological Sciences. The ^3H isotopes were electrolytically enriched and measured using the liquid scintillation counting method with Quantulus-1220 (Pharmacia LKB, Sweden). The results were reported in tritium units (TU), with an analytical precision of ± 2 TU.

3.2 Estimation of residence time of groundwater

The estimation of the mean residence time of the groundwater was done according to the tritium input into the groundwater and the residual tritium measured in the groundwater (Clark and Fritz, 1997). We calculated the mean residence time which was equal to the age of groundwater based on the exponential-piston flow model, which is suitable for aquifers that have regions of confined and unconfined flow model, the measured ^3H concentration at time t (C_t) is connected with the input of ^3H (C_i) via the convolution integral:

$$C_t = \int_0^{\infty} C_i(t-\tau) g(\tau) e^{(-\lambda\tau)} d_\tau \tag{1}$$

where τ represents the residence time, $t-\tau$ is the time when the water recharged, λ is the radioactive decay constant of tracers (^3H, $\lambda = 0.55764\ a^{-1}$), and $g(\tau)$ is the transit time distribution function of flow paths and residence times in the aquifer. For the exponential-piston flow model, $g(\tau)$ is defined as follows (Cartwright and Morgenstern, 2016):

$$g(\tau) = \begin{cases} 0 & \text{for } \tau < T\,(1-f) \\ (fT)^{-1} e^{(-\tau/(ft_t)+1/f-1)} & \text{for } \tau > T\,(1-f) \end{cases} \tag{2}$$

The letter T is meaning of transit time (a) and f is meaning of the ratio of the total volume to the exponential volume in the above equation. When the $f = 0$ the exponential-piston flow model is equivalent to the piston flow model and when the $f = 1$ the exponential-piston flow model is equivalent to the exponential model (Maloszewski and Zuber, 1982; Zuber *et al*., 2005).

When the exponential-piston flow model is used to calculate the mean residence time, the unknown parameters need to be determined first, which is done by the lumped parameter method. Simulations are calibrated to fit the measured ^3H output composition (Jurgens *et al*., 2016; Chatterjee *et al*., 2018; Hagedorn *et al*., 2018). This can be accomplished by numerically integrating the convolution integral (Equation 1). For calculations we used the FLOWPC software (Maloszewski and Zuber 1996).

4 Results and discussion

4.1 Characteristics and composition of hydrochemistry in various water bodies

The physical and chemical parameters of river water and groundwater are shown in Table 1.

The pH of the river water varied from 7.02 to 8.89, averaging as 8.07, which was generally weakly alkaline. The pH value of the river water during the wet season was lower than that of the river water during the dry season. The groundwater pH ranged from 6.49 to 8.37, averaging as 7.66, where the groundwater pH was higher during the dry season. In general, the pH value of river water was higher than that of groundwater. The possible reason might be that the presence of aquatic plants or algae in river water caused the pH value of water to rise (Wang *et al*., 2017). In this study, the TDS value of river water varied from 154 $mg \cdot L^{-1}$ to 936 $mg \cdot L^{-1}$, with an average of 476.76 $mg \cdot L^{-1}$, which signifies fresh water quality. The mean value of river water TDS during the wet season was 296.88 $mg \cdot L^{-1}$. Generally, it was lower than the salinity value in the dry season (mean value 574.25 $mg \cdot L^{-1}$). The low alkaline and TDS values in river water samples indicate that the river water may be affected by glacial snowmelt (Wang *et al*., 2016). Additionally, the TDS values of groundwater varied from 139 $mg \cdot L^{-1}$ to 1782 $mg \cdot L^{-1}$, averaging as 525.8 $mg \cdot L^{-1}$, which was slightly higher than the TDS values of the river. The maximum value of the TDS was found at the QJSW sampling

Table 1 Hydrochemical parameters of water samples in the Zhangjiakou area

Site	Sampling	Water type [a]	Well depth (m)	pH	EC ($us.cm^{-1}$)	TDS ($mg \cdot L^{-1}$)	δD (‰)	$\delta^{18}O$ (‰)	d-excess (‰)
Zhangbei G n=6, S n=3	GJL	G	45	7.41	1014.3	595	–81.80	–11.9	13.8
	ZBM	G	23	7.37	1800.7	1078.8	–76.28	–11.2	13.1
	AGL2	S	/	7.43	1134.3	625.5	–73.02	–11.0	15.0
Sanggan river basin G n=9, S n=3	DTW	G	181	8.16	816.0	463.2	–94.84	–13.4	12.7
	QJSW	G	70	8.07	2398.0	1331.5	–93.06	–13.1	11.5
	HSY	G	41	8.15	394.8	219.6	–81.24	–11.8	12.8
	SGH	S	/	8.16	1019.0	578.0	–73.64	–10.5	10.0
Qingshui river basin G n=18, S n=6	CJ	G	80	7.41	483.0	281.3	–88.33	–13.4	18.9
	DXZ	G	111	7.52	817.7	482.8	–77.84	–11.2	11.7
	ST	G	120	7.42	1002.3	580	–79.74	–11.9	15.1
	QZRL	G	90	7.23	1465.7	835	–77.28	–11.6	15.2
	GS	G	8.55	7.28	658.0	386.7	–80.64	–12.0	15.2
	GJY	G	70	7.14	693.0	417.2	–83.30	–12.5	16.4
	CH	S	/	7.74	328.7	191.0	–83.69	–11.9	11.5
	H1	S	/	8.40	471.3	292.0	–73.82	–10.3	8.9
Yanghe river basin G n=21, S n=15	CG	G	140	7.89	353.6	198.7	–74.91	–10.8	11.7
	DL	G	60	7.75	904.7	531.2	–67.97	–9.7	9.6
	Y1Z	G	103	7.68	585.0	348.2	–74.20	–10.9	12.9
	Y2Z	G	40	7.75	782.0	460.2	–69.15	–10.0	10.6
	XH	G	60	8.05	556.0	325.5	–78.33	–11.5	13.7
	XHY	G	150	7.90	862.4	462.0	–72.60	–10.5	11.6
	NG	G	100	7.86	761.3	461.5	–76.64	–11.2	13.1
	YH	S	/	8.22	738.3	433.7	–69.48	–9.8	9.0
	YX	S	/	8.20	993.0	606.2	–67.54	–9.3	7.1
	YHZ1	S	/	8.02	902.7	530.5	–63.83	–8.7	5.6
	YHZ2	S	/	8.27	710.3	424.5	–71.80	–10.0	8.3
	GT	S	/	8.15	1007.0	609.5	–66.70	–9.2	6.9

[a] G represents groundwater and S surface water.

point located in the Sanggan river basin, which is close to the salt water standard. Definitely, this was partly related to local soil salinization. Besides, TDS and EC data revealed a very good linear relationship (Figure 2) with R^2 = 0.94 (p<0.001), indicating that the parameters measured in the field and lab matched very well. Thus it is justified to use TDS data to represent corresponding changes of EC.

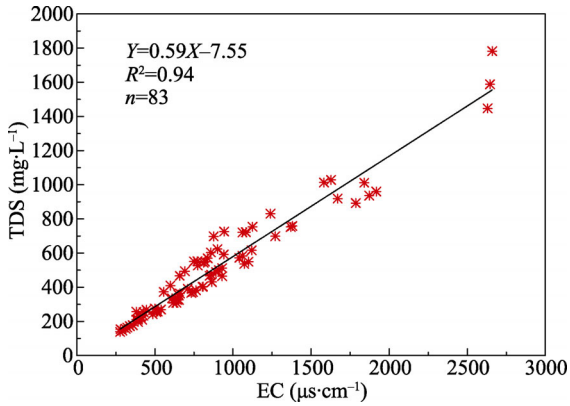

Figure 2 Scatter of plot represented the EC-TDS relationship for all water samples in the Zhangjiakou area

Figure 3 showed the main cations of the river water were Mg^{2+} and Na^{+}, which accounted for 41.85% and 34.94% of the total amount of cations, respectively. Ca^{2+} followed with an average proportion of 21.19%. The order of cation concentrations was Mg^{2+}>Na^{+}>Ca^{2+}>K^{+}. The HCO_3^- was the dominant anion in the river water, accounting for 15.96% – 97.60% of the total anions, with an average ratio of 54.05%. Cl^- followed with an average of 21.98%. The order of anion concentrations was HCO_3^->Cl^->SO_4^{2-}>NO_3^->F^-. Thus, the water chemistry of the river basin were mainly of the HCO_3-Mg·Na type and HCO_3·Cl-Na type.

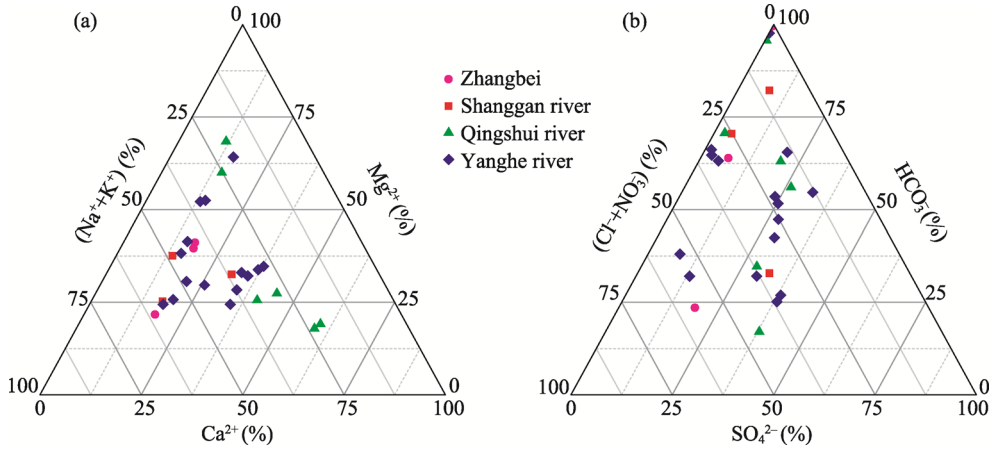

Figure 3 Triangle diagrams showing cation composition (a) and anion composition (b) of the surface water from the Zhangjiakou area

Figure 4 depicts the triangle diagram of groundwater anion and cation in each basin of Zhangjiakou. The main cation in the Zhangbei district were Mg^{2+} and Na^{+}, with the average proportion being 40.27% and 38.56%, respectively. The main anions were HCO_3^- and Cl^-, with an average proportion of 51.99% and 23.92%, respectively. The water chemistry type was mainly HCO_3·Cl-Na and HCO_3·Cl-Mg type. The dominant cations of the groundwater in the Qingshui river basin were Mg^{2+} and Ca^{2+}, with an average proportion of 56.39% and 25.46%, respectively, the main anions were HCO_3^- and SO_4^{2-}, with an average proportion of

64.54% and 13.05%, respectively. The main prevalent chemistry type was HCO_3-Mg·Ca. The dominant cation of the groundwater in the Yanghe river basin was Mg^{2+}, with an average proportion of 50.66%. Ca^{2+} and Na^+ showed almost similar proportions with the average contents of 52.68 mg·L^{-1} and 56.37 mg·L^{-1}, respectively. Anions were mainly HCO_3^- and SO_4^{2-}, with the average proportion of 67.19% and 13.70%, indicating the HCO_3-Mg type for the water chemistry. The concentration of Na^+ and Cl^- of the groundwater in the Sanggan river basin is abnormally high. The average Na^+ concentration is 564.85 mg·L^{-1}, which is the maximum in the Zhangjiakou area. The main cations are Na^+ and Mg^{2+}, with the average proportion of 44.76% and 36.11%, respectively, followed by Ca^{2+}, whose average proportion is 17.90%; the dominant anion was HCO_3^-, and the Cl^- and SO_4^{2-} had the similar proportions of 17.40% and 17.78%, respectively. Collectively, the water chemistry type mainly expressed as HCO_3·Cl·SO_4-Na and HCO_3·Cl·SO_4-Mg type.

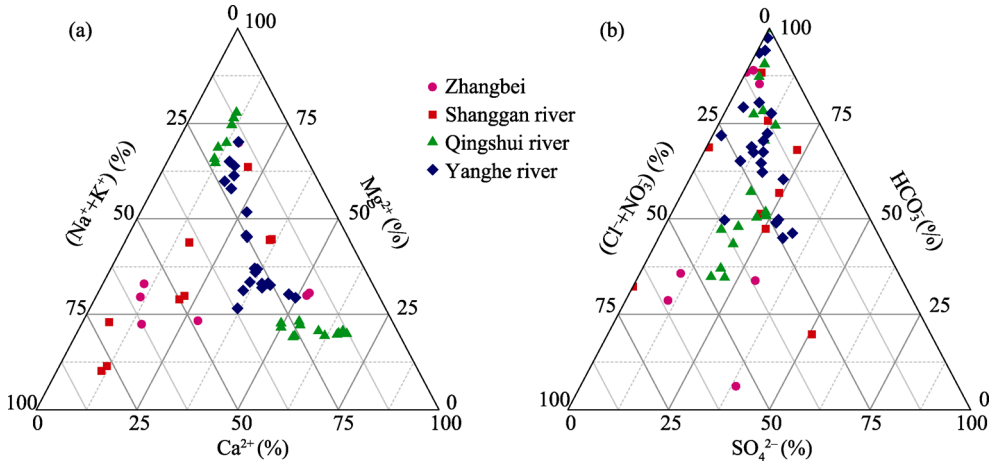

Figure 4 Triangle diagrams showing cation composition (a) and anion composition (b) of the groundwater from the Zhangjiakou area

4.2 Isotope characteristics and seasonal variation of precipitation

The values of δD and $\delta^{18}O$ of the atmospheric precipitation exhibit notable seasonal variation (Table 2). Generally, the δD and $\delta^{18}O$ values were at their maximum in spring, their minimum in winter, and their medium in summer and autumn. This pattern occurs mainly because in spring the water vapor source has a relatively high humidity which produces isotopic depletion. During the winter, the water vapor sources for precipitation are mainly cold and dry continental air masses (Zhu *et al*., 2017). The δD ranged –140.370‰ to +22.058‰, and the $\delta^{18}O$ was –20.393‰ to –0.479‰. According to the global reference values from the International Atomic Energy Agency, the δD was –350‰ to +50‰, the $\delta^{18}O$ was –50‰ to +10‰. In China, the δD was –280‰ to +24‰, the $\delta^{18}O$ was –35.5‰ to +2.5‰ (Tian *et al*., 2001). It is shown that the δD and $\delta^{18}O$ values of precipitation in the Zhangjiakou area were within the expected range.

Based on the δD and $\delta^{18}O$ data of precipitation collected from June 2018 to May 2019 Local Meteoric Water Lines (LMWL) were established as $\delta D = 7.30\ \delta^{18}O + 11.11$ ($R^2 = 0.96$,

Table 2 The precipitation of δD and $\delta^{18}O$ values in 2018 and 2019 in the Zhangjiakou area

Seasons	δD (‰)			$\delta^{18}O$ (‰)		
	Min	Max	Mean	Min	Max	Mean
Spring (March to May)	–89.207	22.058	–41.625	–13.697	–0.479	–7.466
Summer (June to August)	–137.578	–9.806	–63.830	–19.120	–1.381	–10.074
Autumn (September to November)	–140.370	–30.687	–89.519	–20.393	–5.444	–14.149
Winter (December to February)	–124.621	–86.121	–107.781	–18.110	–14.230	–16.251

0.96, n = 52; Figure 5) for the study area. Compared to the GMWL (δD = 8 $\delta^{18}O$ + 10) (Craig, 1961; Zheng *et al*., 1975) and the China atmospheric water line (δD = 7.9 $\delta^{18}O$ + 8.2) (Zheng *et al*., 1982), both the slope (7.30) and the constant term (11.11) were similar, yet with a slightly lower slope and slightly higher constant term, showing an arid area feature.

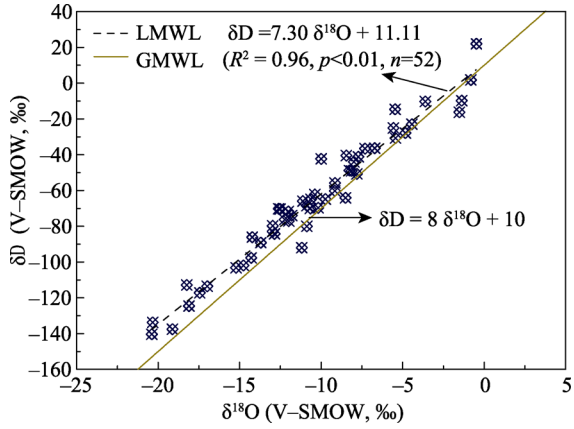

Figure 5 Relationship between δD and $\delta^{18}O$ of precipitation in the Zhangjiakou area. For comparison the Global Meteoric Water Line (GMWL) is presented.

In sub-arid regions, evapotranspiration and subcloud evaporation have obvious impacts on the stable isotopes of local precipitation (Zemp *et al*., 2014; Wang *et al*., 2016b). In general, the lower values of δD and $\delta^{18}O$ might be caused by the recycling of evaporated moisture, while the subcloud evaporation leads to enrichment (Pang *et al*., 2011). Therefore, the LWML in Zhangjiakou area had the smaller slope compared with GMWL, indicating that rainfall isotopic enrichment due to subcloud evaporation over-compensates for isotopic depletion by moisture recycling.

4.3 Isotope characteristics and spatial variation of surface water and groundwater

The average values of $\delta^{18}O$ and δD are shown in Table 1. The isotopic values of the river water samples varied from –86.53‰ to –58.37‰ for δD, averaging as –71.50‰; the variation of $\delta^{18}O$ value was –12.54‰ to –7.09‰, averaging as –10.08‰. According to the δD and $\delta^{18}O$ data of river water samples the Surface Water Line (SWL) equation was modeled as δD =4.43 $\delta^{18}O$ – 26.80 (R^2 = 0.82, n = 27) for Zhangjiakou area. The groundwater isotopes of the δD values varied from –98.63‰ to –62.65‰, averaging as –79.39‰, the $\delta^{18}O$ values varied from –14.62‰ to –7.92‰ with an average of –11.59‰. A cross plot of $\delta^{18}O$ and δD of the groundwater samples is used to develop a Groundwater Line (GWL) as δD = 4.92 $\delta^{18}O$ – 22.39 (R^2 = 0.85, n = 56) for the study area (Figure 6). The slope of the GWL was 4.92, and hence much lower than that of the LMWL (7.30) but was slightly higher than that of the SWL (4.43), which is a typical phenomenon in semi-arid areas (Wen *et al*., 2005). The similarity compositions among surface water and groundwater suggested a good hydrological connection in the study area. Furthermore, the slopes of the SWL and GWL were close to each other and less than LMWL, implying the groundwater received recharge mostly from surface waters and partly from direct precipitation (Hao *et al*., 2019).

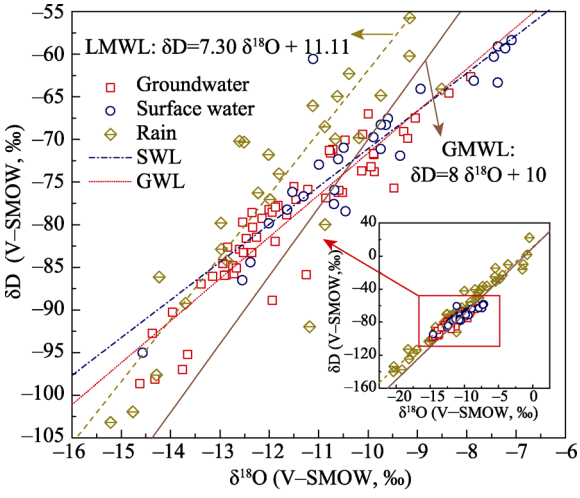

Figure 6 The δD and $\delta^{18}O$ distributions of groundwater samples along with surface water samples in Zhangjiakou area

According to the data of groundwater collected from each basin in the Zhangjiakou area, a GWL was established for each region as follows: $\delta D = 4.34\ \delta^{18}O - 28.58$ ($R^2 = 0.88$) [Zhangbei], $\delta D = 4.99\ \delta^{18}O - 26.03$ (R^2=0.85) [Sanggan], $\delta D = 3.79\ \delta^{18}O - 35.49$ ($R^2 = 0.85$) [Qingshui], $\delta D = 4.12\ \delta^{18}O - 29.54$ ($R^2 = 0.88$) [Yanghe]. Furthermore, the slope of Sanggan GWL (4.99) was slightly higher than that of GWL (4.92), the GWL slope for the other three basins was smaller than that of GWL, but all the values of slope were close to that of the GWL. Both regression lines for SWL and GWL have a lower slope than the GMWL and a negative intercept, suggesting an important effect of evaporative enrichment on groundwater (Wassenaar *et al*., 2011).

4.4 Deuterium excess

The d-excess is a useful parameter and commonly applied to study the sources of water vapor and the evaporation effect during rainfall (Gat 1983; Clark and Fritz, 1997). The deuterium excess (d-excess), defined by d-excess = $\delta D - 8\times\delta^{18}O$ quantifies the surplus deuterium about Craig's line (Dansgaard, 1964). In the Zhangjiakou area the d-excess of precipitation samples varied largely from –4.16‰ to +37.71‰, averaging as 18.45‰ (Table 1). The d-excess values of river water samples varied from –4.40‰ to +28.30‰, averaging as 9.14‰. The d-excess of groundwater samples also varied largely from +0.09‰ to +22.20‰, averaging 13.36‰. Most samples had higher d-excess values (10.75‰ to 37.71‰) than the intercept of GMWL (10‰), except the values measured during snowmelt (–4.40‰ to 9.97‰). This indicates that the primary evaporation was controlled by the low humidity of the vapor sources (Kendall and McDonnell, 1998). Both d-excess in samples of QJSW (4.13‰) and DTW (5.13‰) were relatively lower, where are from artesian wells in the Sanggan river basin. The two particular groundwater presented high TDS (1446.5 mg/L and 1588 mg/L), high concentration of Cl^- and Na^+ in the study area. They might be attributed by the water-rock interactions with a deep groundwater circulation, which allowed these two samples characterized by a $\delta^{18}O$-shift-like change.

4.5 Tritium concentrations in groundwater

Tritium (^3H) is a useful radioistope to distinguish groundwater recharged during the pre-bomb time from younger water with its half-life of 12.43 a, especially to identify the modern recharge of groundwater (Clark and Fritz, 1997; Newman *et al*., 2010; Clark, 2015). The ^3H concentration in groundwater varied from detection limit (<2 TU) to 10.57 TU, averaging as 4.97 TU (Figure 7). The sample of ZBM in Zhangbei had the largest ^3H content (10.57 TU) in the study area, indicating the groundwater in ZBM may be mainly affected by

atmospheric precipitation. Apart from this, the values of ^{3}H in the rest samples were less than 8 TU. Most samples exhibited higher ^{3}H concentrations than 2 TU, suggesting that the groundwater is recharged by modern water of less than 60 years. These ^{3}H concentrations varied vertically with depth, and showed a clear decline with depth (Figure 7). The groundwater samples collected above 50 m showed a much broader range values of ^{3}H concentration (2.06 to 10.57 TU, 5.62±2.70), the groundwater samples between 50 to 100 m showed a smaller range of ^{3}H concentration variation (<2 to 6.94 TU, 4.32±2.10), the groundwater samples collected from more than 100 m showed a minimum range of ^{3}H concentration variation (<2 to 4.36, 2.68±1.05). The ^{3}H concentration in Qingshui river basin has the largest range of variation, while the ^{3}H concentration in Sanggan river basin presented the smallest range varying from detection limit (<2 TU) to 2.06 TU. The ^{3}H values of 3 samples from depths below 100 m were <2 TU, which implies that the ^{3}H concentration of groundwater at 100 m is the background level of stratum. Groundwater had a relatively low tritium in the confined aquifers, indicating that the groundwater might be recharged before 1952 (Guo *et al*., 2019).

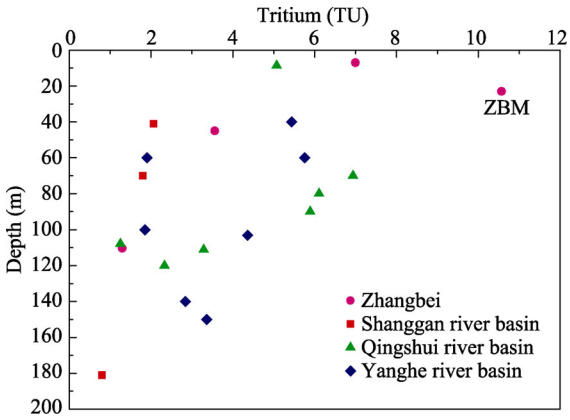

Figure 7 Variation of ^{3}H concentrations with sampling depths in different river basins

4.6 Residence time of groundwater and recharge rates

For the Zhangjiakou area, the best fit of the exponential piston flow model was found for f ranging between 0.7 and 0.9 and the transit time t. Accordingly, the calculated groundwater age varied between 25 and 60 years (Figure 8). The corresponding groundwater age of most samples was more than 60 years. The sample of ZBM in Zhangbei might be modern water due to its lower determined age of 22 years (Figure 8).

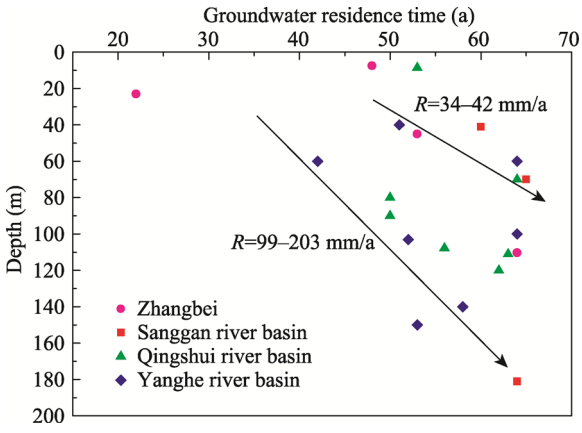

Figure 8 The relationship between groundwater residence times calculated from the ^{3}H concentrations using the exponential piston flow model with depth in the Zhangjiakou area. The lower line with arrow indicates Yanghe river basin and Qingshui river basin, the upper line with arrow indicates Zhangbei and Sanggan river basin.

The mean residence time of groundwater can be used to evaluate the recharge rates based on the assumption that the groundwater flow paths in the aquifers are steep so that groundwater residence times correlate with depth without lateral position (Ian and Uwe, 2012). The relationship between groundwater residence time and the depth (Figure 8) indicates that the in-

terpretation of recharge rates from residence times is valid. Particularly, the ^{3}H residence time of groundwater samples was positively correlated with depth from the Yanghe river basin and Qingshui river basin. The vertical velocity of groundwater from these two basins was calculated to be 1.1 to 2.26 m/a. In turn, the corresponding recharge rates were estimated to be 0.99–0.203 m/a (99–203 mm/a) taking into account of their investigated soil porosity of 0.09 (The data from Geological Survey report for Zhangjiakou). Soil texture and porosity in the Zhangbei and in the Sanggan river basin are different from the Yanghe river basin and Qingshui river basin (Geological survey report for Zhangjiakou). Hence, the vertical velocity was estimated to be 1.71 to 2.1 m/a, and the recharge rates were 0.034–0.042 m/a (34–42 mm/a) in the Zhangbei and the Sanggan river basin. The groundwater age and recharge rates are very important indicators to evaluate renewability regime of groundwater, and this can provide useful information for the sustainable use of groundwater.

5 Conclusions

This study explained the spatial and temporal variation of the stable isotope (δD, $\delta^{18}O$) composition in groundwater, river and precipitation and adopted the radioisotope (^{3}H) to estimate the age of groundwater in the Zhangjiakou area. Furthermore, the mean residence times and recharge rates were calculated using the exponential-piston flow model. Results showed that the LMWL exhibited different slopes and intercepts compared with the GMWL, partly due to isotopic depletion caused by over-compensation of subcloud evaporation. The groundwater in the region is strongly connected with the local meteoric water. Based on the tritium concentrations varying with depth, the age of groundwater ranged from 25 years to more than 60 years and groundwater generally above 100 m might be the modern water, younger than 60 years. However, we assumed groundwater below 100 m to be a mixture of modern and old water. Furthermore, the recharge rates ranged from 0.034 to 0.203 m/a. This study has still several limitations of insufficient data such as more isotopic data and potential influencing factors since the discharge of groundwater is complex, more isotopic sampling and analysis of potential influencing factors are needed in further study. More studies on this subject are therefore necessary to manage precisely groundwater resources in the Zhangjiakou area, North China.

References

Ansari M A, Sharma S, Kumar U S *et al*., 2014. Hydrogeological controls of radon in a few hot springs in the Western Ghats at Ratnagiri district in Maharashtra India. *Current Science*, 107(9): 1587–1590.

Cao C, Li X Y, 2019. Temporal and spatial characteristics and density of agriculture and animal husbandry of the water footprint at the district and county scales: A case study of Zhangjiakou city. *China Rural Water and Hydropower*, (4): 124–131. (in Chinese)

Cao W G, Yang H F, Liu C L *et al*., 2018. Hydrogeochemical characteristics and evolution of the aquifer systems of Gonghe Basin, northern China. *Geoscience Frontiers*, 9(3): 907–916.

Chatterjee S, Sinha U K, Ansari M A *et al*., 2018. Application of lumped parameter model to estimate mean transit time (MTT) of the thermal water using environmental tracer (^{3}H): Insight from Uttarakhand geothermal area (India). *Applied Geochemistry*, 94: 1–10.

Chen Z, Jiang W G, Wang W J *et al*., 2017. The impact of precipitation deficit and urbanization on variations in water storage in the Beijing-Tianjin-Hebei urban agglomeration. *Remote Sensing*, 10(1): 1–12.

Clark I D, 2015. Groundwater Geochemistry and Isotopes. FL, USA: CRC Press Boca Raton.

Clark I D, Fritz P, 1997. Environmental Isotopes in Hydrogeology. New York: Lewis, 328 p.

Craig, 1961. Isotopic variation in meteoric waters. *Science*, 133: 1702–1703.

Dansgaard W, 1964. Stable isotopes in precipitation. *Tellus*, 16 (4): 436–446.
Döll P, Hoffmann-Dobrev H, Portmann F T *et al*., 2012. Impact of water withdrawals from groundwater and surface water on continental water storage variations. *Journal of Geodynamics*, 59/60: 143–156.
Feng W, Zhong M, Lemoine J M *et al*., 2013. Evaluation of groundwater depletion in North China using the Gravity Recovery and Climate Experiment (GRACE) data and ground-based measurements. *Water Resources Research*, 49(4): 2110–2118.
Foster S, Chilton P, 2003. Groundwater: The processes and global significance of aquifer degradation. *Philosophical Transactions of the Royal Society of London*: *Series B*, *Biological Sciences*, 358(1440): 1957–1972.
Gat J R, 1983. Palaeoclimates and Palaeowaters: A Collection of Environmental Isotope Studies. In: Proceedings of an Advisory Group Meeting on the Variations of the Isotopic Composition of Precipitation and of Groundwater During the Quaternary as a Consequence of Climatic Changes, IAEA.
Gibson J, Birks S, Yi Y, 2016. Stable isotope mass balance of lakes: A contemporary perspective. *Quaternary Science Reviews*, 131: 316–328.
Gleeson T, Befus K M, Jasechko S *et al.*, 2015. The global volume and distribution of modern groundwater. *Nature. Geoscience*, 9(2): 161–167.
Guo C Y, Shi J S, Zhang Z J *et al*., 2019. Using tritium and radiocarbon to determine groundwater age and delineate the flow regime in the Taiyuan Basin, China. *Arabian Journal of Geosciences*, 12: 185.
Gusyev M A, Morgenstern U, Stewart M K *et al*., 2016. Application of tritium in precipitation and river water in Japan: A case study of groundwater transit times and storage in Hokkaido watersheds. *Hydrology and Earth System Sciences*, 20(7): 3043–3058.
Hagedorn B, Clarke N, Ruane M *et al*., 2018. Assessing aquifer vulnerability from lumped parameter modeling of modern water proportions in groundwater mixtures: application to California's south coast range. *Science of the Total Environment*, 624: 1550–1560.
Hao S, Li F D, Li Y H *et al*., 2019. Stable isotope evidence for identifying the recharge mechanisms of precipitation, surface water, and groundwater in the Ebinur Lake basin. *Science of the Total Environment*, 657: 1041–1050.
Hou L, Peng W Q, Qu X D *et al*., 2019. Runoff changes based on dual factors in the upstream area of Yongding river basin. *Polish Journal of Environmental Studies*, 28(1): 143–152.
Huang T, Pang Z, 2010. China: Evidence from environmental isotopes and water chemistry. *Journal of Hydrology*, 387(3): 188–201.
Huang T M, Pang Z H, Li J *et al*., 2017. Mapping groundwater renewability using age data in the Baiyang alluvial fan, NW China. *Hydrogeology Journal*, 25(3): 743–755.
Ian C, Uwe M, 2012. Constraining groundwater recharge and the rate of geochemical processes using tritium and major ion geochemistry: Ovens catchment, southeast Australia. *Journal of Hydrology*, 475(1): 137–149.
Jurgens B C, Böhlke J K, Kauffman *et al*., 2016. A partial exponential lumped parameter model to evaluate groundwater age distributions and nitrate trends in long-screened wells. *Journal of Hydrology*, 543(5): 109–126
Kalbus E, Reinstorf F, Schirmer M, 2006. Measuring methods for groundwater-surface water interactions: A review. *Hydrology and Earth System Science*, 10(6): 873–887.
Kamtchueng B T, Fantong W Y, Wirmvem M J *et al*., 2015. A multi-tracer approach for assessing the origin, apparent age and recharge mechanism of shallow groundwater in the lake Nyos catchment, northwest, Cameroon. *Journal of Hydrology*, 523: 790–803.
Kendall C, McDonnell J J, 1998. Isotope Tracers in Catchment Hydrology. Amsterdam, The Netherlands: Elsevier Science.
Li A J, Schmitz O J, Stephan S *et al*., 2015. Photocatalytic transformation of acesulfame: Transformation products identification and embryotoxicity study. *Water Research*, 89: 68–75.
Liu J, Chen Z Y, Wei W *et al*., 2014. Using chlorofluorocarbons (CFCs) and tritium (^{3}H) to estimate groundwater age and flow velocity in Hohhot basin, China. *Hydrological Processes*, 28(3): 1372–1382.
Maloszewski P, Zuber A, 1982. Determining the turnover time of groundwater systems with the aid of environmental tracers: 1. Models and their applicability. *Journal of Hydrology*, 57(3): 207–231.
Maloszewski P, Zuber A, 1996. Lumped parameter models for the interpretation of environmental tracer data, chap. 2 in International Atomic Energy Agency. In: Manual on Mathematical Models in Isotope Hydrogeology, TECDOC-910.
Michel R L, 2004. Tritium hydrology of the Mississippi River basin. *Hydrology Process*, 18(7): 1255–1269.
Morgenstern U, Daughney C J, 2012. Groundwater age for identification of baseline groundwater quality and impacts of land-use intensification: The National Groundwater Monitoring Programme of New Zealand.

Journal of Hydrology, 456/457: 79–93.

Newman B D, Osenbrück K, Aeschbach H *et al*., 2010. Dating of 'young' groundwater using environmental tracers: Advantages, applications, and research needs. *Isotopes Environmental Health Studies*, 46: 259–278.

Pang Z H, Kong Y L, Klaus F *et al*., 2011. Processes affecting isotopes in precipitation of an arid region. *Taylor Journal*, 63(3): 352–359.

Perry E, Paytan A, Pedersen B *et al*., 2009. Groundwater geochemistry of the Yucatan Peninsula, Mexico: Constraints on stratigraphy and hydrogeology. *Journal of Hydrology*, 367(1): 27–40.

Shao P, Wang L L An J L *et al*., 2012. Observation and analysis of air pollution in Zhangjiakou, Hebei. *Environmental Science*, 33(8): 2538–2550. (in Chinese)

Sun P L, Xu Y Q, Wang S, 2014. Terrain gradient effect analysis of land use change in poverty area around Beijing and Tianjin. *Transactions of the Chinese Society of Agricultural Engineering*, 30(14): 277–288. (in Chinese)

Tian L D, Yao T D, Sun W Z *et al*., 2001. Relationship between δD and $\delta^{18}O$ in precipitation from north to south of the Tibetan Plateau and moisture cycling. *Science in China* (*Series D*: *Earth Sciences*), 44(9): 789–796.

Tian Y, Xu Y Q, Guo H F *et al*., 2012. Simulation of farmland use pattern in Zhangjiakou based on multinomial logistic regression model. *Resources Science*, 34(8): 1493–1499. (in Chinese)

Tipple B J, 2017. Stable hydrogen and oxygen isotopes of tap water reveal structure of the San Francisco Bay Area's water system and adjustments during a major drought. *Water Research*, 119: 212–224.

Wada Y, Van beek L P H, Bierkens M F P, 2012. Nonsustainable groundwater sustaining irrigation: A global assessment. *Water Resources Research*, 48(6): 2055–2072.

Wang C X, Dong Z W, Qin X *et al*., 2016. Glacier meltwater runoff process analysis using δD and $\delta^{18}O$ isotope and chemistry at the remote Laohugou glacier basin in western Qilian Mountains, China. *Journal of Geographical Sciences*, 26(6): 722–734.

Wang P, Hu G, Cao J H, 2017. Stable carbon isotopic composition of submerged plants living in karst water and its eco-environmental importance. *Aquatic Botany*, 140: 78–83.

Wang S J, Zhang M J, Chen Y J *et al*., 2016. Contribution of recycled moisture to precipitation in oases of arid central Asia: A stable isotope approach. *Water Resources Research*, 52(4): 3246–3257.

Wang X, Ma F B, Li C H *et al*., 2015. A Bayesian method for water resources vulnerability assessment: A case study of the Zhangjiakou region, North China. *Physics and Chemistry of the Earth*, 47(2): 99–113.

Wen X, Wu Y, Su J *et al*., 2005. Hydrochemical characteristics and salinity of groundwater in the Ejina basin, northwestern China. *Environmental Geology*, 48: 665–675.

Xu W, Su X S, Dai Z X *et al*., 2017. Multi-tracer investigation of river and groundwater interactions: A case study in Nalenggele River basin, northwest China. *Hydrogeology Journal*, 25(7): 2015–2029.

Yangui H, Abidi I, Zouari K *et al*., 2012. Deciphering groundwater flow between the complex terminal and plio-Quaternary aquifers in Chott Gharsa Plain (southwestern Tunisia) using isotopic and chemical tools. *Hydrological Sciences Journal*, 57(5): 967–984.

Yao T C, Zhang X P, L I G *et al*., 2016. Characteristics of the stable isotopes in different water bodies and their relationships in surrounding areas of Yuelu mountain in the Xiangjiang river basin. *Journal of Natural Resources*, 31(7): 1198–1210. (in Chinese)

Yi Y, Gibson J J, Hélie J-F *et al*., 2010. Synoptic and time-series stable isotope surveys of the Mackenzie River from Great Slave Lake to the Arctic Ocean, 2003 to 2006. *Journal of Hydrology*, 383(3/4): 223–232.

Yuan F, Mayer B, 2012. Chemical and isotopic evaluation of sulfur sources and cycling in the Pecos River, New Mexico, USA. *Chemical Geology*, 291: 13–22.

Yurtsever Y, 1975. Worldwide Survey of Stable Isotope in Precipitation. Vienna: IAEA.

Zemp D C, Schleussner C F, Barbosa H M J *et al*., 2014. On the importance of cascading moisture recycling in South America. *Atmospheric Chemistry and Physics*, 14: 13337–13359.

Zhang B, Song X F, Zhang Y H *et al*., 2017. The renewability and quality of shallow groundwater in Sanjiang and Songnen plain, northeast China. *Journal of Integrative Agriculture*, 16(1): 229–238.

Zheng S H, Hou F G, Ni B L, 1982. Study on the meteoric hydrogen and oxygen isotope in China. *Science Bulletin*, 13: 801–806.

Zhu Y W, Zhang F P, Wang H W *et al*., 2017. Analysis on characteristics of stable hydrogen and oxygen isotopes in precipitation in Shijiazhuang. *Shandong Agricultural Sciences*, 49(5): 116–123. (in Chinese)

Zuber A, Witczak S, Rozanski K *et al*., 2005. Groundwater dating with ^{3}H and SF6 in relation to mixing patterns, transport modelling and hydrochemistry. *Hydrological Process*, 19(11): 2247–2275.